AIAA 82-4298

Improved Solution of Optimal Impulsive Fixed-Time Rendezvous

Frank C. Liu*
University of Alabama, Huntsville, Alabama
and
Larry D. Plexico†
U.S. Army Missile Command, Redstone Arsenal, Alabama

A linear approach to the minimum-fuel problem of fixed-time multi-impulse rendezvous between vehicles on close circular orbits has proven to be simple and convenient. It deals with the linearized motion of the active vehicle relative to a reference point moving on a circular reference orbit. This paper shows that the normalized characteristic velocity is invariant with respect to each choice of reference orbit in the domain of normalized initial angular difference-normalized rendezvous time. Numerical examples are used to demonstrate the adaptability of linear solutions to the nonlinear case by means of a hybrid method. It is shown that the proposed mean velocity reference orbit more accurately describes the impulse locations and magnitudes than does the mean radius reference orbit.

Nomenclature

a = semimajor axis
A,B,C = constants in the primer vector equations
e = eccentricity of orbit
g = gravity acceleration vector
p = primer vector
r = radius of orbit
r_A = initial orbit radius of active vehicle
r_r = radius of reference orbit
r_T = target orbit radius
δR = normalized distance between inner and outer orbits, Eq. (8)
δr = radial deviation divided by r_r
t = time
t_F = total time of flight
U = unit vector in direction of thrust
v_r = orbital velocity of reference orbit
Δv = characteristic velocity
Δv^* = normalized characteristic velocity, $\Delta v/\delta R$
Δv_T = total velocity impulse magnitude
W = matrix in Eq. (25)
W_i = ith column of W
x = state vector
δ = variation of a parameter or a variable
δx = variation of the state vector
$\delta\bar{x}$ = defined by Eq. (18)
η = initial central angle between reference position and target
η_r = equivalent initial angle on reference orbit
η_r^* = normalized initial angle, $\eta_r/\delta R$
θ = central angle
μ = gravitational constant
λ,μ,ν = components of primer vector
τ = normalized time in revolution of reference orbit
ϕ = state transition matrix

Subscripts

F = final value
i = ith impulse
0 = initial condition
r = reference orbit
T = target or total value

Received Dec. 11, 1981; revision received April 22, 1982.

*Professor, Department of Mechanical Engineering. Member AIAA.
†Aerospace Engineer.

Introduction

PROBLEMS dealing with minimum fuel, multiple-impulse, fixed-time rendezvous of vehicles between two close circular orbits are of great interest to aerospace engineers for mission planning. Numerous papers dealing with this special case of the Lawden's problem[1] were published in the 1960's; some related to this study are given in Refs. 2-10. Hoelker and Silber[2] treated the bielliptic transfer consisting of three impulses which for some geometries require less fuel than the Hohmann transfer. Robbins[3] investigated the consumption difference between finite thrust solutions and impulsive solutions, and arrived at a performance penalty. It was found that the impulsive approximation provides a good estimate for fuel requirements for high thrust rockets. A linearized analysis of the noncoplanar, neighboring orbit transfer problems was addressed by Edelbaum.[4] It presented a class of singular solutions which consists of an infinite number of possibilities for the distribution of impulses. A different approach to the impulsive transfer problems was developed by Breakwell.[5] The state was assumed to be composed of the orbital elements with the control being the location and direction of the impulse. Expressions were derived which relate variations in orbital parameters to velocity perturbations. Breakwell and Heine[6] applied the Pontryagin maximum principle to a special case involving neighboring noncoplanar elliptical orbits. Optimal solutions consisting of two- and three-impulse transfer trajectories were presented. The extension of the primer vector concept to nonoptimal trajectories by Lion and Handelsman[7] resulted in the establishment of necessary conditions for the inclusion of additional interior impulses, as well as for initial or final coasts.

Far less attention has been given to optimal multiple-impulse fixed-time rendezvous trajectories than to time open transfers. A technique for determining optimum transfer and rendezvous trajectories between two arbitrary states of position and velocity was described by Jezewski and Rozendaal.[8] Prussing[9,10] applied Lawden's theory of the primer vector to neighboring orbits, linearizing the equations of motion about an intermediate orbit. The construction of the primer vector locus (which determines times and direc-

tions of the impulses) is handled separately from the boundary-value problem (which determines velocity impulse magnitudes). Optimal two- to four-impulse solutions were formulated for rendezvous between coplanar circular orbits.

The method of linear solution for optimal multiple-impulse, fixed-time circle-to-circle coplanar rendezvous developed by Prussing offers a simple and attractive tool to obtain approximate orbital transfer data. Prussing uses a point moving on a circular reference orbit as a reference point. The radius of the reference orbit is taken as the mean value of the target and active vehicle orbital radii. Although the mean radius orbit is a simple and convenient choice of reference, it may not be an ideal one to obtain the best result. For instance, if one considers an active vehicle rendezvous with a target on an outside orbit with a large lead angle, a large portion of the transfer trajectory lies inside the initial orbit of the active vehicle. Thus, the central angle between the active vehicle and the reference point increases with time. The velocity increments required for orbital transfer are sensitive to position error of the impulse points. This raises the question of the effectiveness of the linear solution to be used for the construction of an actual optimal transfer trajectory.

One objective of this study is to introduce a reference orbit which minimizes the angular position error of the impulse points. The reference point moving on an orbit which has the mean velocity of the active vehicle during the transfer will accomplish this. In this case, the reference point will remain close to the active vehicle in angle and coincides with it at the initial and rendezvous times. Another objective of this investigation is to show that the normalized velocity increment required for rendezvous is independent of the reference orbit radius. Numerical examples are used to compare results based on the two reference orbits; also a study of the effectiveness of these linear solutions is made using a hybrid technique.

Analysis

Perturbed Motion Relative to a Point Moving on a Circular Orbit

The equations of orbital motion of a particle under gravitational force are

$$r\ddot{\theta}+2\dot{r}\dot{\theta}=0 \tag{1a}$$

$$\ddot{r}-r\dot{\theta}^2=-\mu/r^2 \tag{1b}$$

where the overdot denotes differentiation with respect to time, r and θ are, respectively, the radial distance from the center of attraction and angular displacement, and μ is the gravitational constant. From Eqs. (1) a set of equations for a perturbed motion from a circular motion are derived, after linearization,

$$a\delta\ddot{\theta}+2\omega\delta\dot{r}=0 \tag{2a}$$

$$\delta\ddot{r}-2a\omega\delta\dot{\theta}-3\omega^2\delta r=0 \tag{2b}$$

where δ denotes small perturbation of the state variables, and a and ω are the radius and angular velocity of the circular orbit, respectively. Thus, the equations of motion of a particle relative to reference point moving on a circular orbit are

$$x''+2y'=0 \tag{3a}$$

$$y''-2x'-3y=0 \tag{3b}$$

$$z''+z=0 \tag{3c}$$

where x, y, and z are tangential, radial, and normal components. The prime denotes differentiation with respect to τ where $\tau=\omega t$. Note that x, y, and z are normalized with respect to orbital radius, and x', y', and z' are normalized with respect to orbital velocity. The solution of the state variables in matrix form is

$$\begin{bmatrix} x \\ y \\ z \\ x' \\ y' \\ z' \end{bmatrix} = \begin{bmatrix} 1 & -6(\tau-\sin\tau) & 0 & -3\tau+4\sin\tau & -2(1-\cos\tau) & 0 \\ 0 & 4-3\cos\tau & 0 & 2(1-\cos\tau) & \sin\tau & 0 \\ 0 & 0 & \cos\tau & 0 & 0 & \sin\tau \\ 0 & -6(1-\cos\tau) & 0 & -3+4\cos\tau & -2\sin\tau & 0 \\ 0 & 3\sin\tau & 0 & 2\sin\tau & \cos\tau & 0 \\ 0 & 0 & -\sin\tau & 0 & 0 & \cos\tau \end{bmatrix} \begin{bmatrix} x_0 \\ y_0 \\ z_0 \\ x_0' \\ y_0' \\ z_0' \end{bmatrix} \tag{4}$$

Equation of Primer Vector along a Circular Orbit

The differential equation of the adjoint variables of an orbital motion under gravitational force is

$$\ddot{p}=Gp \tag{5}$$

where boldface type represents a vector and the gravity gradient matrix $G=\partial g/\partial r$. Vector p, the so-called primer vector, has radial, circumferential, and normal components (λ,μ,ν) respectively. For a particle moving on a circular orbit, Eq. (5) reduces to identical form as Eq. (3). Hence, the solution for the in-plane components is

$$\lambda=A(\cos\tau+2B) \tag{6a}$$

$$\mu=A(C-2\sin\tau-3B\tau) \tag{6b}$$

The arbitrary constants A, B, and C must be determined such that Lawden's necessary conditions[1] are satisfied. These conditions for optimal impulsive orbit transfer are as follows.

1) The primer and its first time derivative must be continuous everywhere.

2) The impulsive thrust must be aligned with primer vector and is applied when $p=1$.

3) The magnitude of the primer is less than or equal to unity during the transfer.

4) At all junction points not at the terminals, $p=0$.

Note that 1) constant C locates the origin of the $\mu-\lambda$ axis, 2) constant A determines the size of the μ-λ locus, and 3) at any junction point the dot product of the vector (μ,λ) with itself is unity and with its derivative is zero. These constants may be computed by using a simple single variable search technique.[11] Since primer vector locus plots can be found elsewhere,[9] the μ-λ locus will not be presented here.

Choices of Reference Orbits and Boundary Conditions

1. Mean Radius Reference Orbit

The reference orbit used by Prussing[9,10] is designated as the mean radius reference orbit (MRR) and it has a radius,

$$r_r=\tfrac{1}{2}(r_A+r_T) \tag{7}$$

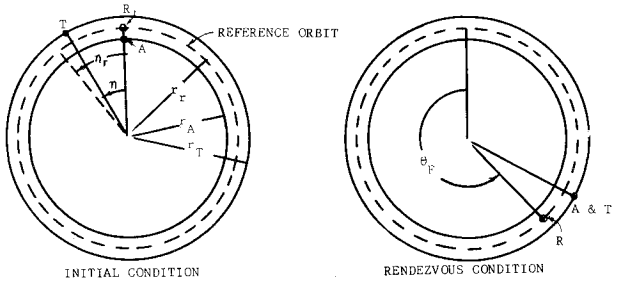

a)

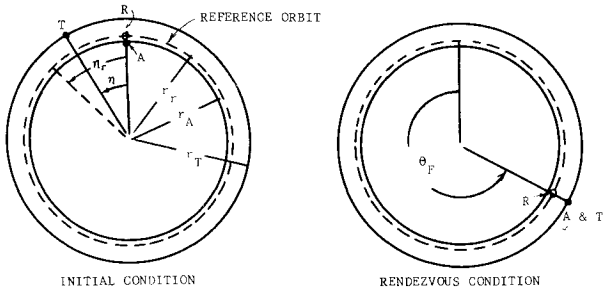

b)

Fig. 1 Rendezvous geometry and boundary conditions; a) mean radius reference orbit and b) mean velocity reference orbit.

and

$$\delta R = (r_T - r_A)/r_r \tag{8}$$

where r_A and r_T are, respectively, orbital radii of the active and target vehicles. Applying the variation of angular velocity of orbital motion,

$$\delta\omega = -\frac{3}{2}\sqrt{\mu}a^{-5/2} = -\frac{3}{2}\omega\delta a/a$$

and setting the semimajor axis a equal to r_r and $\delta a/a$ equal to $-\frac{1}{2}\delta R$, one obtains the expression for the variation of the initial state variable θ' of the active vehicle with respect to the reference point moving on the reference orbit, $\delta\theta' = \frac{3}{4}\delta R$. As shown in Fig. 1a, the variation of the initial state is

$$\delta x_0 = \begin{bmatrix} \delta\theta \\ \delta r \\ \delta\theta' \\ \delta r' \end{bmatrix}_{\tau=0} = \begin{bmatrix} 0 \\ -\frac{1}{2}\delta R \\ \frac{3}{4}\delta R \\ 0 \end{bmatrix} \tag{9}$$

Let η denote the initial lead angle of the target vehicle with respect to the reference point. Based on equal time of flight, an equivalent angle η_r of an imaginary target on the reference orbit (where $\eta_r/\omega_r = \eta/\omega_T$) is obtained

$$\eta_r = \eta(r_T/r_r)^{3/2} \tag{10}$$

The variation of the final state of the active vehicle with respect to the reference point at the time of rendezvous is

$$\delta x_F = \begin{bmatrix} \delta\theta \\ \delta r \\ \delta\theta' \\ \delta r' \end{bmatrix}_{\tau=\tau_F} = \begin{bmatrix} \eta_r - \frac{3}{4}\delta R\tau_F \\ \frac{1}{2}\delta R \\ -\frac{3}{4}\delta R \\ 0 \end{bmatrix} \tag{11}$$

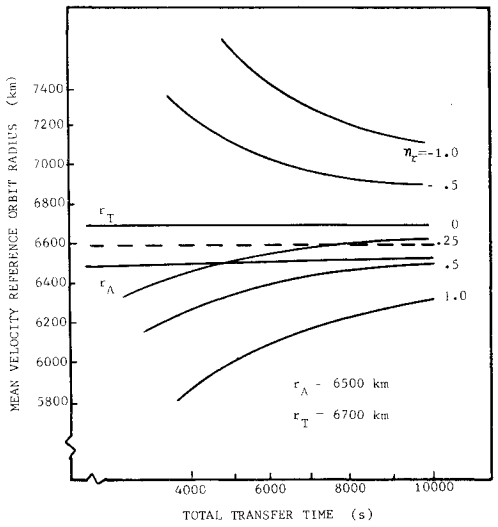

Fig. 2 MVR orbit radius vs transfer time.

2. Mean Velocity Reference Orbit

This paper presents an alternate choice of reference orbit which has an angle velocity equal to the average angular velocity of the active vehicle during the transfer time. As shown in Fig. 1b, the final angle at rendezvous is

$$\theta_F = \eta + \sqrt{\mu/r_T^3}t_F = \sqrt{\mu/r_r^3}t_F \tag{12}$$

Therefore, the radius of the mean velocity reference orbit (MVR) is

$$r_r = [\mu(t_F/\theta_F)^2]^{1/3} \tag{13}$$

Figure 2 illustrates r_r for the MVR orbit vs transfer time for a given set of values $r_A = 6500$ km and $r_T = 6700$ km. Note that r_r may fall inside of r_A when η has a large positive value, or outside r_T when η has a large negative value.

By inspecting Fig. 1b, one readily may write the variations of the initial and final states of the active vehicle with respect to the reference point as follows.

$$\delta x_0 = \begin{bmatrix} 0 \\ -\delta R + \frac{2}{3}\eta_r/\tau_F \\ 3/2\delta R - \eta_r/\tau_F \\ 0 \end{bmatrix} \tag{14}$$

and

$$\delta x_F = \begin{bmatrix} 0 \\ \frac{2}{3}\eta_r/\tau_F \\ -\eta_r/\tau_F \\ 0 \end{bmatrix} \tag{15}$$

Determination of Change of Velocity

The variation of state of the active vehicle with respect to the reference point at time τ_i due to the variation of initial state and increment of velocity at τ_j may be written in the form

$$\delta x_i = \phi_{i0}\delta x_0 + \sum_{j=1}^{n}\phi_{ij}\delta x_j \tag{16}$$

where the vector δx_j has components $(0,\Delta v_j)$, ϕ_{i0} and ϕ_{ij} are the state transition matrices, and n is the number of impulses. Hence, the variation of the final state is

$$\delta x_F = \phi_{F0}\delta x_0 + \sum_{j=1}^{n} [\phi_{FjA}\phi_{FjB}] \begin{bmatrix} 0 \\ \Delta v_j \end{bmatrix} \tag{17}$$

which may be rewritten in the form

$$\delta\tilde{x} = \delta x_F - \phi_{F0}\delta x_0 = \sum_{j=1}^{n} \phi_{FjB}\Delta v_j \tag{18}$$

where, from Eq. (4)

$$\phi_{F0} = \begin{bmatrix} 1 & 6(\tau_F - \sin\tau_F) & 4\sin\tau_F - 3\tau_F & 2(\cos\tau_F - 1) \\ 0 & 4 - 3\cos\tau_F & 2(1-\cos\tau_F) & \sin\tau_F \\ 0 & 6(\cos\tau_F - 1) & 4\cos\tau_F - 3 & -2\sin\tau_F \\ 0 & 3\sin\tau_F & 2\sin\tau_F & \cos\tau_F \end{bmatrix} \tag{19}$$

The development of Eq. (18) from which the Δv magnitudes are obtained parallels that in Refs. 9 and 10. Now, it can be shown that Eq. (18) is independent of the choice of reference orbit. Substitution of Eqs. (9) and (19) for the MRR orbit, and Eqs. (14) and (19) for the MVR orbit, into Eq. (18), respectively, yields identical results

$$\delta\tilde{x} = \begin{bmatrix} \eta_r - 3/2\delta R\tau_F \\ \delta R \\ -3/2\delta R \\ 0 \end{bmatrix} \tag{20}$$

This implies that the solution of Δv_j from Eq. (18) is a function of the parameters η_r and τ_F which are normalized with respect to the chosen reference orbit and the normalized Δv_j are independent of the choice of the reference orbit.

1. Two-Impulse Rendezvous

For a fixed-time, two-impulse transfer the exact solution can be obtained by solving Lambert's problem. It provides a basis for direct comparison of the total velocity increment obtained from the linear solution. The transition matrix of Eq. (18) reduces to

$$\phi_{F1B} = \begin{bmatrix} \phi_A \\ \hline \phi_B \end{bmatrix} = \left[\begin{array}{cc} 4\sin\tau_F - 3\tau_F & 2(\cos\tau_F - 1) \\ 2(1-\cos\tau_F) & \sin\tau_F \\ \hline 4\cos\tau_F - 3 & -2\sin\tau_F \\ \sin\tau_F & \cos\tau_F \end{array}\right] \tag{21}$$

$$\phi_{F2B} = \begin{bmatrix} 0 \\ I \end{bmatrix} \tag{22}$$

Solving Δv from Eq. (18), one obtains

$$\begin{bmatrix} \Delta v_1 \\ \Delta v_2 \end{bmatrix} = \begin{bmatrix} \phi_A^{-1} & 0 \\ -\phi_B\phi_A^{-1} & I \end{bmatrix} \delta\tilde{x} \tag{23}$$

The components of the primer vector can be computed from

$$\lambda_j = \Delta v_{jr}/\Delta v_j \qquad \mu_j = \Delta v_{j\theta}/\Delta v_j \qquad j = 1,2 \tag{24}$$

2. Three-Impulse Rendezvous

Rewrite Eq. (18) in the form

$$\delta\tilde{x} = W\Delta v \tag{25}$$

and define the jth column of W matrix by

$$W_j = \phi_{FjB}U_j \tag{26}$$

where U_j is a unit vector in the direction of the jth impulsive thrust. The transition matrix ϕ_{FjB} in Eq. (26) is similar to Eq. (21) in which τ_F is replaced by $\tau_F - \tau_j$ with $j = 1$, 2, and 3. If the determinant of the matrix $[\delta x W]$ vanishes, a unique solution of Δv is obtained,

$$\begin{aligned} \Delta v_1 &= \delta R(KW_{22} - W_{21})/S_{12} \\ \Delta v_2 &= \delta R(W_{11} - KW_{12})/S_{12} \\ \Delta v_3 &= -\delta R(KS_{42} + S_{14})S_{12}U_{3r} \end{aligned} \tag{27}$$

where $K = \eta_r/\delta R - (3/2)\tau_F$ and $S_{ij} = W_{1i}W_{2j} - W_{1j}W_{21}$.

3. Four-Impulse Rendezvous

The solution of Δv can be obtained from Eq. (25) by matrix inversion,

$$\Delta v = W^{-1}\delta x \tag{28}$$

Regions of Optimal Two-, Three-, and Four-Impulse Transfers

The optimal value of the total velocity increment Δv required by fixed-time rendezvous for a given leading angle η can be presented by plotting the normalized η_r^*, $\eta_r/\delta R$, vs τ_F with Δv^* (i.e., the normalized quantity $\Delta v/\delta R$) as a parameter. Formulation of the equation of the boundaries that define the two-, three-, and four-impulse regions is given here.

1. Boundaries of Four-Impulse Region

The case of a three-impulse transfer with an initial coast may be considered as a four-impulse case with the magnitude of the first impulse approaching to zero. By letting Δv_1 from Eq. (28) equal zero, results in the equation of the boundary locus separating the four impulse and the three impulse with initial coast

$$\eta_r^* = \frac{(3/2S_{12} - S_{31})U_{r4} + S_{41}U_{\theta 4}}{S_{23}U_{r4} - S_{42}U_{\theta 4}} + \frac{3}{2}\tau_F = \eta_r/\delta R \tag{29}$$

As the rendezvous time is increased in the four-impulse region, the magnitude of Δv_2 gradually diminishes to zero when the right-hand side boundary separating the four-impulse and the three-impulse region is reached. The plot of regions is given in Fig. 3.

2. Boundary Between Three Impulse and Three Impulse with Initial Coast

The three impulse with initial coast is bounded by the four-impulse region on the right, the two impulse with initial coast below, and the three impulse on the left. The constant Δv^* contour lines are straight lines in this region, increasing linearly with transfer time. That is to say, the cost of transfer is not changed due to an initial coast. An initial coast simply allows a phase correction to take place prior to a regular three-impulse transfer. That is, a given initial lead angle and a specified transfer time cannot satisfy the requirement for an

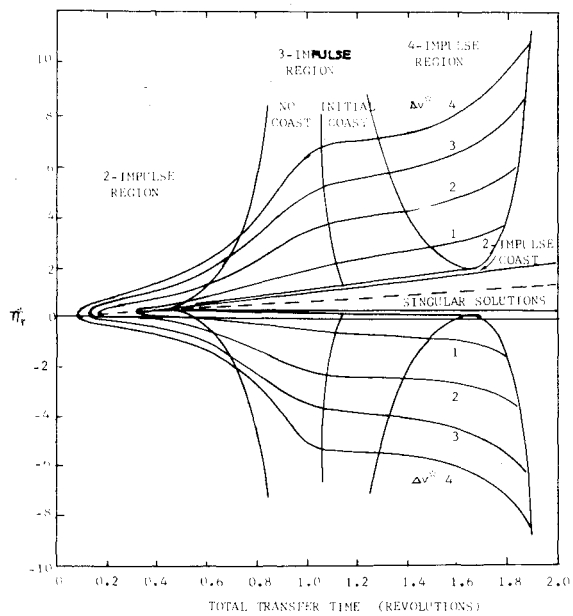

Fig. 3 Regions of optimal multiple impulse solutions.

optimal three-impulse transfer without initial coast. Allowing an initial coast of time $(\tau_1 - \tau_0)$ yields a new lead angle at the first impulse,

$$\eta_1 = \eta - \tfrac{3}{4}\delta R(\tau_1 - \tau_0) \tag{30}$$

The angle η_1 decreases linearly with coast time until such conditions are reached that allow an optimal three-impulse transfer.

3. Boundary of Three-Impulse Region

As the second impulse of the three-impulse transfer trajectory becomes unnecessary for optimality, the magnitude of the primer vector will at this point drop below unity, and an optimal two-impulse solution will result. Making Δv_2 given by the second equation of Eq. (27) equal to zero, one obtains the equation of the boundary locus separating the three-impulse and two-impulse regions,

$$\eta_r^* = W_{11}/W_{12} + \frac{3}{2}\tau_F \tag{31}$$

In a similar manner, the boundary between the regions of the three impulse and the two impulse with an initial coast is determined by letting Δv_1 given by Eq. (27) equal to zero. This leads to the equation of the boundary locus

$$\eta_r^* = W_{21}/W_{22} + \frac{3}{2}\tau_F \tag{32}$$

4. Region of Degenerate Solutions

A singular arc occurs when the magnitude of the primer vector is unity during the entire transfer and, hence, impulse times are not uniquely defined. The transfer trajectories within this region (see Fig. 3) may consist of two-impulse transfers with initial and/or final coast, or multiple-impulse transfers, and they all have equal Δv_T. Note that $p = 1$ is satisfied at all time if $\lambda = 0$ and $\mu = 1$. That is, all impulses are applied circumferentially. To satisfy the earlier described conditions the only admissible solution for Eq. (23) is that $\tau_2 - \tau_1 = (2n-1)\pi$, when n is an integer, $\Delta v_1 = \Delta v_2 = \frac{1}{4}\delta R$, and $\eta = \frac{3}{4}(2n-1)\pi\delta R$. The total cost, $\Delta v_T = \frac{1}{2}\delta R$, is equal to the cost of a Hohmann transfer. The shape of the singular region is a wedge. The upper boundary of the wedge which has a slope of 3/2 represents rendezvous solutions consisting of an initial coast and a Hohmann transfer. The lower

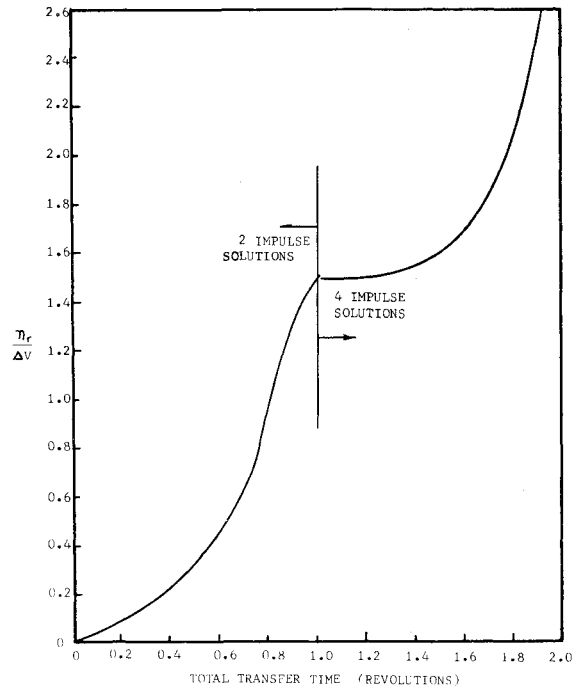

Fig. 4 Optimal solutions for $\delta R = 0$.

boundary is a line $\eta_r^* = 3/8$. It should be pointed out that a region of singular solutions could consist of multiple-impulse cases, and with sufficiently long transfer time a rendezvous trajectory could consist of two or more Hohmann transfers.

Extension of Region to Negative Value of η_r^*

All the regions of optimal transfers described are presented in Fig. 3. It has been assumed that η_r^* is positive; that is η_r and δR are either both positive or both negative. Now, consider the case for negative η_r^* and take a pair of points in the (η_r^*, τ_F) domain; P and $\bar{P}$, which have equal distance above and below the line $\eta_r^* - \frac{3}{4}\tau_F = 0$. This is to say, $\bar{\eta}_r^* = 3/2\tau_F - \eta_r^*$. Thus, the first element on the right-hand side of Eq. (20) is replaced by $-\eta_r$. It follows from Eq. (18) that

$$\Delta v_T(\eta_r^*, \tau_F) = \Delta \bar{v}_T(\bar{\eta}_r^*, \tau_F) \tag{33}$$

Using the two-impulse case as an example, it can be shown that Eq. (23) results in

$$\Delta \bar{v}_{1\theta} = \Delta v_{2\theta} \qquad \Delta \bar{v}_{1r} = -\Delta v_{2r}$$

$$\Delta \bar{v}_{2\theta} = \Delta v_{1\theta} \qquad \Delta \bar{v}_{2r} = -\Delta v_{1r}$$

and, hence, $\Delta \bar{v}_T = \Delta v_T$. This shows that all the regions and the constant η_r^* contour lines can be extended from a point above the line defined by $\eta_r^* - \frac{3}{4}\tau_F = 0$, to a point of equal distance below the line.

It is significant to point out the region boundaries plotted in Fig. 3 are obtained from a somewhat different viewpoint than that given in Ref. 10. It is in complete agreement with Prussing's work. A simple transformation between Fig. 3 and his work is given by the first equation of Eq. (11), namely

$$\delta\theta_F/\delta R - \eta_r^* - \tfrac{3}{4}\tau_F \tag{34}$$

Rendezvous of Vehicles on the Same Orbit

When both the target and the active vehicles are on the same orbit, the components of $\delta\bar{x}$ to be used for the determination of Δv are $(\eta_r, 0, 0, 0)$. It is noted that there exists no optimal three-impulse rendezvous solution.

Table 1 Example I: two-impulse rendezvous

$r_A = 6578$ km, $r_T = 6978$ km, $\eta = 28.37$ deg, $t_F = 3088$ s

Reference orbit	MRR	MVR	Exact orbit $a = 6655$ km $e = 0.0722$
r_r, km	6778	6364	
v_r, m/s	7669	7914	
τ_F, rro[a]	0.556	0.611	
η_r, rro	0.0823	0.0905	
Δv_1, m/s	604	589	559
Δv_2, m/s	545	461	441
Δv_T, m/s	1080	1050	1000
Δv^*	0.142	0.133	
$\eta_r/\Delta v$	0.58	0.68	
% Error of Δv_T	8	5	

[a] Revolutions of the reference orbit.

Table 2 Example II: two-impulse rendezvous on the same orbit

$r_A = r_T = 6778$ km, $\eta = 33.8$ deg, $t_F = 3692$ s

Reference orbit	MRR	MVR	Exact orbit $a = 6419$ km $e = 0.0816$
r_r, km	6778	6135	
v_r, m/s	7669	8060	
τ_F, rro[a]	0.665	0.772	
η_r, rro	0.0939	0.109	
Δv_1, m/s	621	531	500
Δv_2, m/s	621	531	500
Δv_T, m/s	1242	1062	1000
$\Delta v = \Delta v_T / v_r$	0.162	0.132	
$\eta_r/\Delta v$	0.58	0.83	
% Error of Δv_T	24.2	6.2	

[a] Revolutions of the reference orbit.

Table 3 Example III: four-impulse rendezvous with small lead angle

$r_A = 6744$ km, $r_T = 6812$ km, $\eta = 28.6$ deg, $t_F = 8088$ s

Reference orbit	MRR	MVR
r_r, km	6778	6572
v_r, m/s	7669	7788
$\delta R = (r_T - r_A)/r_r$	0.010	0.0103
η_r, rro[a]	0.080	0.084
τ_F, rro	1.4565	1.525
η_r^*	4.38	4.09
	First impulse	
t_1, s (rro)	0 (0)	0 (0)
$\delta\theta_1$, deg (rro)	0 (0)	0 (0)
δr_1	−0.005	0.0263
Δv_1, m/s	46	55
Δv_1 (hybrid), m/s	46	58
	Second impulse	
t_2, s (rro)	1930 (0.3476)	2108 (0.3975)
$\delta\theta_2$, deg (rro)	2.25 (0.006)	3.57 (0.010)
δr_2	−0.024	−0.001
Δv_2, m/s	102	89
Δv_2 (hybrid), m/s	114	94
	Third impulse	
t_3, s (rro)	6159 (1.109)	5975 (1.127)
$\delta\theta_3$, deg (rro)	23.31 (0.062)	4.03 (0.011)
δr_3	−0.032	−0.0057
Δv_3, m/s	98	97
Δv_3 (hybrid), m/s	104	101
	Fourth impulse	
t_4, s (rro)	8088 (1.4565)	8088 (1.525)
$\delta\theta_4$, deg (rro)	24.87 (0.069)	0 (0)
δr_4	0.005	0.0366
Δv_4, m/s	88	86
Δv_4 (hybrid), m/s	88	90
Δv_T, m/s	336	328
Δv_T (hybrid), m/s	393	343
$\Delta v = \Delta v_T / v_r$	0.0438	0.0421
$\Delta v^* = \Delta v / \delta R$	4.38	4.09

[a] Revolutions of the reference orbit.

Table 4 Example IV: four-impulse rendezvous with large lead angle and radial distance

$r_A = 6642$ km, $r_T = 6912$ km, $\eta = 111.8$ deg, $t_F = 8088$ s

Reference orbit	MRR	MVR
r_r, km	6778	6057
v_r, m/s	7669	8100
$\delta R = (r_T - r_A)/r_r$	0.0398	0.0444
η_r, rro[a]	0.3198	0.377
τ_F, rro	1.4565	1.7254
η_r^*	8.035	8.49
	First impulse	
t_1, s (rro)	0 (0)	0 (0)
$\delta\theta_1$, deg (rro)	0 (0)	0 (0)
δr_1	0.02	0.1013
Δv_1, m/s	185	371
Δv_1 (hybrid), m/s	199	342
	Second impulse	
t_2, s (rro)	1930 (0.3476)	2538 (0.5411)
$\delta\theta_2$, deg (rro)	9.0 (0.021)	1.45 (0.003)
δr_2	−0.098	−0.063
Δv_2, m/s	407	217
Δv_2 (hybrid), m/s	6872	205
	Third impulse	
t_3, s (rro)	6159 (1.109)	5555 (1.1842)
$\delta\theta_3$, deg (rro)	93.22 (0.021)	5.54 (0.003)
δr_3	−0.129	−0.090
Δv_3, m/s	397	332
Δv_3 (hybrid), m/s	6353	331
	Fourth impulse	
t_4, s (rro)	8088 (1.4565)	8088 (1.7254)
$\delta\theta_4$, deg (rro)	99.48 (0.276)	0 (0)
δr_4	0.02	0.146
Δv_4, m/s	352	442
Δv_4 (hybrid), m/s	362	403
Δv_T, m/s	1341	1362
Δv_T (hybrid), m/s	13786	1282
$\Delta v = \Delta v_T / v_r$	0.1749	0.1681
$\Delta v^* = \Delta v / \delta R$	4.394	3.78

[a] Revolutions of the reference orbit.

1. Two-Impulse Case

The velocity increments for two-impulse transfer from Eq. (23) are

$$\Delta v_1 = \Delta v_2 = \frac{[\sin^2\tau_F + 4(\cos\tau_F - 1)^2]^{1/2}}{8(1-\cos\tau_F) - 3\tau_F \sin\tau_F}\eta_r \qquad (35)$$

Optimal two-impulse transfers are limited to transfer times of up to one orbital revolution. Figure 4 presents a plot of $\eta_r/\Delta v$ vs τ_F. It is seen that for a given initial angle η, Δv decreases as the total flight time increases.

2. Four-Impulse Case

For transfer times between 1 and about 1.9 orbital revolutions, the optimal rendezvous requires four impulses. It is noted that $\Delta v_1 = \Delta v_4$ and $\Delta v_2 = \Delta v_3$. Numerical results are shown in Fig. 4.

Hybrid Method of Solution to Transfer Trajectories

It is important to determine the adaptability of a linear solution to rendezvous problems and also to compare results based on the two different reference orbits. Analytical solutions can be obtained only for the two-impulse case to provide a basis for direct comparison. One approach is to apply the computed data (impulse times and Δv's) from a linear solution to construct a patched conic transfer trajectory and determine the miss distance at rendezvous time. Since rendezvous requires matching velocity of the vehicles, the miss distance alone is not a suitable criterion. Another ap-

Table 5 Additional numerical results from example IV

	MRR			Hybrid solution based on MRR					
t_i, s	λ	μ	Δv_i, m/s	λ	μ	Δv_i, m/s	a,[a] km	e [b]	θ,[c] deg
0	−0.1742	−0.9847	185	0.133	−0.991	199	6324	0.050	134
1930	−0.0542	−0.9985	407	0.894	−0.449	6872	5681	0.753	358
6159	−0.0542	0.9985	397	−0.867	0.498	6353	6324	0.093	131
8088	−0.1742	0.9847	352	−0.016	0.999	362	6912	0	–
	MVR			Hybrid solution based on MVR					
0	−0.3449	−0.9386	371	−0.232	−0.972	342	6126	0.085	197
2538	−0.0475	−0.9989	217	0.290	−0.957	205	5826	0.050	236
5555	−0.0475	0.9989	332	0.353	0.935	331	6309	0.100	190
8088	−0.3449	0.9386	442	−0.375	0.927	403	6912	0	–

[a] a = semi-major axis. [b] e = eccentricity of conic. [c] θ = central angle.

Table 6 Example V: four-impulse rendezvous with large lead angle and radial distance—target vehicle on inner orbit

$r_A = 6912$ km, $r_T = 6642$ km, $\eta = 118.7$ deg, $t_F = 8088$ s

Reference orbit	MRR	MVR
r_r, km	6778	5819
v_r, m/s	7669	8276
$\delta R = (r_T - r_A)/r_r$	−0.0398	−0.0464
η_r, rro[a]	0.3198	0.427
τ_F, rro	1.4565	1.831
η_r^*	−8.036	−9.198
	First impulse	
t_1, s (rro)	0 (0)	0 (0)
$\delta\theta_1$, deg (rro)	0 (0)	0 (0)
δr_1	0.02	0.202
Δv_1, m/s	438	687
Δv_1 (hybrid), m/s	458	620
	Second impulse	
t_2, s (rro)	1930 (0.3476)	2711 (0.6137)
$\delta\theta_2$, deg (rro)	8.59 (0.018)	4.67 (0.012)
δr_2	−0.165	−0.051
Δv_2, m/s	524	270
Δv_2 (hybrid), m/s	1615	326
	Third impulse	
t_3, s (rro)	6159 (1.109)	5379 (1.7177)
$\delta\theta_3$, deg (rro)	119.51 (0.267)	−14.67 (−0.036)
δr_3	−0.135	−0.078
Δv_3, m/s	534	127
Δv_3 (hybrid), m/s	609	162
	Fourth impulse	
t_4, s (rro)	8088 (1.4565)	8088 (1.831)
$\delta\theta_4$, deg (rro)	131.78 (0.363)	0 (0)
δr_4	−0.02	0.1555
Δv_4, m/s	271	633
Δv_4 (hybrid), m/s	296	575
Δv_T, m/s	1767	1717
Δv_T (hybrid), m/s	2978	1683
$\Delta v = \Delta v_T / v_r$	0.2304	0.2075
$\Delta v^* = \Delta v / \lvert\delta R\rvert$	5.789	4.472

[a] Revolutions of the reference orbit.

proach is to use the computed data (time and location of impulses) from a linear solution and connect these locations by conic arcs. This involves solving Lambert's problem to determine the Δv's required for each arc. The second approach, referred to as the hybrid method, is adopted here, because rendezvous of the vehicles is realized. Furthermore, the hybrid method is one step closer to a true optimal solution than is the linear solution. Several numerical examples will be presented to demonstrate the effectiveness of a linear solution based on two different reference orbits.

Numerical Examples

The input data for all six examples presented in Tables 1-8 are radial distances for both vehicles, the initial central angle between the vehicles, and the rendezvous time. It is considered that the target vehicle is leading the active vehicle and that the target is on the outside orbit except in example V (Tables 6 and 7). Two examples deal with rendezvous between vehicles on the same orbit: a two-impulse case (example II, Table 2) and a four-impulse case (example VI, Tables 4 and 5). Rendezvous with small initial lead angles are: two impulse (example II, Table 2) and four impulse (example III, Table 3). Rendezvous with large initial lead angles are: target vehicle on outside orbit (example IV, Tables 4 and 5) and active vehicle on outside orbit (example V, Tables 6 and 7), both require four impulses. Examples III-VI (Tables 3-8) all have transfer times of 8088 s.

A close examination of the unrealistic velocity changes for the MRR-hybrid case ($\Delta v_2 = 6872$ m/s and $\Delta v_3 = 6353$ m/s) is made to determine the cause of the breakdown in the use of parameters from the linear case. One finds from the tabulated data that the segment between the second and third impulses has central angle $\theta = 358$ deg, radial difference $= 0.031\ r_r$, and time of flight $= 0.761$ reference orbital period. To satisfy these conditions requires abnormal velocity changes at the beginning and the end of the arc with eccentricity $e = 0.753$. Figures 5 and 6 illustrate the impulse positions by using the MRR and MVR orbits, respectively.

Table 7 Additional numerical results from example V

	MRR			Hybrid solution based on MRR					
t_i, s	λ	μ	Δv_i, m/s	λ	μ	Δv_i, m/s	a,[a] km	e[b]	θ,[c] deg
0	−0.1742	−0.9847	438	0.0464	−0.9989	458	6190	0.117	135
1930	−0.0542	−0.9985	524	0.9293	−0.3693	1615	5366	0.112	385
6159	−0.0542	0.9985	534	−0.0775	0.9770	609	6185	0.074	138
8088	−0.1742	0.9847	271	0.1847	0.9828	296	6642	0	–
	MVR			Hybrid solution based on MVR					
0	0.4131	−0.9107	687	−0.4171	−0.9089	620	6054	0.146	225
2711	0.0418	−0.9991	270	0.4080	−0.9130	326	5636	0.136	198
5379	0.0418	0.9991	127	0.5163	0.8564	162	5824	0.141	235
8088	0.4131	0.9107	633	−0.1825	0.9832	575	6642		–

Table 8 Example VI: four-impulse on the same orbit

$r_A = 6778$ km, $r_T = 6778$ km, $\eta = 36$ deg, $t_F = 8088$ s

Reference orbit	MRR	MVR
r_r, km	6778	6484
v_r, m/s	7669	7841
$\delta R = (r_T - r_A)/r_r$	0	0
η_r, rro[a]	0.100	0.1069
τ_F, rro	1.4565	1.556
	First impulse	
t_1, s (rro)	0 (0)	0 (0)
$\delta\theta_1$, deg (rro)	0 (0)	0 (0)
δr_1	0	0.4085
Δv_1, m/s	97	114
Δv_1 (hybrid), m/s	98	112
	Second impulse	
t_2, s (rro)	1930 (0.3476)	2178 (0.419)
$\delta\theta_2$, deg (rro)	−2.57 (−0.007)	−4.83 (−0.013)
δr_2	−0.041	−0.0087
Δv_2, m/s	145	140
Δv_2 (hybrid), m/s	162	139
	Third impulse	
t_3, s (rro)	6159 (1.109)	5899 (1.1349)
$\delta\theta_3$, deg (rro)	33.15 (0.086)	4.88 (0.013)
δr_3	−0.041	−0.0087
Δv_3, m/s	145	140
Δv_3 (hybrid), m/s	162	139
	Fourth impulse	
t_4, s (rro)	8088 (1.4565)	8088 (1.556)
$\delta\theta_4$, deg (rro)	36 (0.100)	0 (0)
δr_4	0	0.0458
Δv_4, m/s	97	114
Δv_4 (hybrid), m/s	98	112
Δv_T, m/s	484	508
Δv_T (hybrid), m/s	520	502
$\Delta v = \Delta v_T / v_r$	0.0631	0.0648
η_r / Δ_v	1.585	1.649

[a] Revolutions of the reference orbit.

Observations

Based on the numerical examples, the following observations are made.

1) Linear solutions using the MRR and MVR methods are comparable in terms of Δv_T estimation, with the latter being typically more accurate.

2) For the cases of rendezvous with large initial lead angles (examples IV and V), the hybrid solutions based on the MRR data yield very large Δv's. This is caused by the large variation of the position vector at the impulse points as illustrated in Fig. 5. The MVR method allows the active vehicle and the moving reference point to remain close during the entire transfer time as shown in Fig. 6. The large Δv is due to the large radial velocity component needed for a highly elliptic transfer conic arc.

3) It is significant to note that the last four examples were chosen to have the same transfer time and the same mean radii of the vehicles. Therefore, the MRR method yields identical impulse times for all four cases of different starting geometry. This is not the case for the more accurate MVR method.

Conclusions

1) All the parameters for optimal impulse rendezvous between two close circular orbit (impulse times and thrust vectors) are functions of the normalized parameters, η_r^* and τ_F, whose values are dependent on the choice of the reference orbit. The results mapped in Fig. 3 can be used for both the MRR and MVR orbits.

2) The MRR orbit method can be used for Δv_T estimation, but when the predicted impulse times are applied to construction of transfer conic arcs, it may lead to large errors if the initial separtation of the vehicles is not small.

3) The application of the MVR orbit is simple and it offers better accuracy.

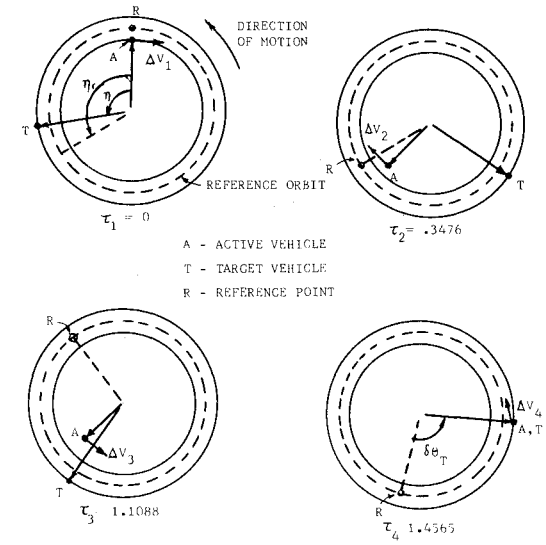

Fig. 5 Rendezvous history with MRR orbit.

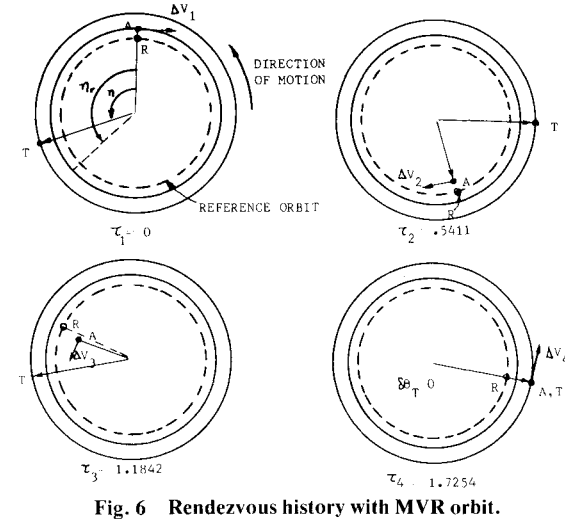

Fig. 6 Rendezvous history with MVR orbit.

References

[1] Lawden, D.F., *Optimal Trajectories for Space Navigation,* Butterworth, London, 1963.

[2] Hoelker, R.E. and Silber, R., "The Bi-Elliptic Transfer Between Coplanar Circular Orbits," *Proceedings of the 4th AFMBD/STL Symposium,* Vol. 3, 1961, pp. 164-175.

[3] Robbins, H.M., "Analytical Study of the Impulsive Approximation," *AIAA Journal,* Vol. 4, Aug. 1966, pp. 1417-1423.

[4] Edelbaum, T.N., "Minimum Impulse Transfer in the Vicinity of a Circular Orbit," *Journal of the Astronautical Sciences,* Vol. 14, March-April 1967, pp. 66-73.

[5] Breakwell, J.V., "Minimum Impulse Transfer Between a Circular Orbit and a Nearby Non-coplanar Elliptic Orbit," *Proceedings of the Colloquium on Optimization in Space Flight Mechanics,* Liege, Belgium, 1967, pp. 155-276.

[6] Breakwell, J.V. and Heine, W., "Minimum Impulse, Time Free Transfer Between Neighboring Noncoplanar Elliptic Orbits with Major Axes Perpendicular to the Line of Nodes," *AIAA Journal,* Vol. 7, July 1969, pp. 1236-1241.

[7] Lion, P.M. and Handelsman, M., "Primer Vector on Fixed Time Impulsive Trajectories," *AIAA Journal,* Vol. 8, Jan. 1968, pp. 127-132.

[8] Jezewski, D.T. and Rozendaal, H.L., "An Efficient Method for Calculating Optimal Free-Space N-Impulse Trajectories," *AIAA Journal,* Vol. 6, Nov. 1968, pp. 2160-2165.

[9] Prussing, J.E., "Optimal Four-Impulse Fixed-Time Rendezvous," *AIAA Journal,* Vol. 4, Aug. 1966, pp. 1417-1423.

[10] Prussing, J.E., "Optimal Two- and Three-Impulse Fixed-Time Rendezvous in the Vicinity of a Circular Orbit," *AIAA Journal,* Vol. 8, July 1970, pp. 1221-1228.

[11] Plexico, L.D., "Optimal Rendezvous Between Close Circular Orbits," PhD Dissertation, The University of Alabama in Huntsville, Huntsville, Ala., May 1980.